Optical Switching and Networking ▮ (▮▮▮▮) ▮▮▮–▮▮▮

Contents lists available at ScienceDirect

Optical Switching and Networking

journal homepage: www.elsevier.com/locate/osn

Regeneration savings in flexible optical networks with a new load-aware reach maximization ☆

A. Bononi [a,*], P. Serena [a], A. Morea [b], G. Picchi [a]

[a] Dip. Ingegneria dell' Informazione, Università degli Studi di Parma, Viale G. P. Usberti 181/A, 43124 Parma, Italy
[b] Alcatel-Lucent Bell Labs France, Route de Villejust, 91620 Nozay, France

ARTICLE INFO

Article history:
Received 6 November 2014
Received in revised form
17 March 2015
Accepted 2 July 2015

Keywords:
Coherent detection
Gaussian Noise model
Dispersion-uncompensated networks

ABSTRACT

We propose and analyze a new load-aware reach maximization procedure based on the Gaussian Noise model for dispersion-uncompensated optical networks with coherent detection. We estimate the opto-electronic regeneration savings with respect to the standard full-load reach approach, and find examples where significant savings can be achieved. The load aware reach and its corresponding optimal power can be computed in real time by the routing and wavelength assignment unit to make statistical decisions about setting-up new lightpaths or regenerating existing ones.

1. Introduction

This paper addresses the physical layer design of flexible optical networks [1–8] and its interplay with the routing layer. In such circuit-switched dispersion uncompensated (DU) fiber-optic networks, wavelength division multiplexed (WDM) dual polarization (DP) optical digital signals are transmitted and coherently detected. Each fiber carries at most W wavelengths with possibly mixed modulation formats. From the source, the destination may be transparently reached via a single lightpath at a specific wavelength without opto-electronic regeneration (OER), or through a concatenation of lightpaths on possibly different wavelengths, with OER from one lightpath to the next one. To minimize the number of costly OERs, the quality-of-transmission (QoT) aware routing and wavelength assignment (RWA) unit first tries to set-up a circuit along a single lightpath. A connection may be unfeasible for two reasons: (i) unavailability of the same wavelength across successive fibers along the lightpath, leading to *wavelength blocking* (WB); (ii) the received signal to noise ratio (SNR) for the considered modulation format is below a required minimum S_0, leading to *SNR blocking* (SB).

In this paper, which is an extension of [9], we concentrate on the SB due to accumulation of linear and nonlinear optical impairments [1,6,3,7,8]. The standard approach is to set-up only lightpaths whose physical length is below the *full-load (FL) reach*, i.e., the maximum length guaranteeing a received SNR above S_0 when all W wavelengths on all fibers are occupied. The FL reach is used as a lightpath-length threshold above which intermediate regenerations are introduced, regardless of the actual wavelength load, i.e., the fraction of wavelengths actually utilized along the current lightpath. Using the FL reach is clearly conservative, since wavelengths saturation at the network core prevents the wavelength load to reach unity. In this paper, we propose a new power selection and OER regeneration strategy where the reach is maximized at the actual wavelength load, and quantify the potential OER savings with respect to using the FL reach and the power selection strategy suggested in [6]. The analysis in the present paper is based on the Gaussian Noise (GN) model for DU coherent links [10,6–8].

☆ Invited paper.

* Corresponding author.
E-mail address: alberto.bononi@unipr.it (A. Bononi).

http://dx.doi.org/10.1016/j.osn.2015.07.003
1573-4277/

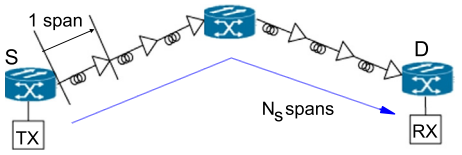

Fig. 1. Sketch of selected reference lightpath from source S to destination D across N_s spans. $H=2$ hops and $\mathcal{S}=3$ span/hop in the example.

The paper is organized as follows. Section 2 briefly recalls the expression of the received electrical SNR that includes nonlinearity according to the GN model, and defines the SB events. Section 3 introduces the key ideas of the new load-aware reach maximization procedure and anticipates the main numerical results of this paper. Section 4 then provides the full analytical details behind the numerical results. Conclusions are finally drawn in Section 5.

2. Nonlinear transmission model

We focus on the transparent transmission of a DP signal across a *reference* lightpath from source to destination, as depicted in Fig. 1. A lightpath is a sequence of H *hops* across access nodes (i.e., add-drop nodes where circuits may originate and terminate), where the hop k is a concatenation of $\mathcal{S}_k$ amplified spans followed by the crossing of the k-th intermediate node, for $k=1,\ldots,H$. A *span* is composed of a transmission fiber followed by an end-line lumped optical amplifier. A *node* is composed of a wavelength demultiplexer, an add/drop block, a possible switching block, and an output multiplexer.[1] In our calculations, the losses in crossing a node are assumed to be equivalent to those in crossing one span.

The reference lightpath is composed of $N_s=\sum_{k=1}^{H}\mathcal{S}_k$ spans. We assume that each of the $W-1$ remaining wavelengths of hop k carries an interferer lightpath (hence carries power) with known probability u_k, $k=1,\ldots,H$. Such wavelength utilization probabilities (or *loads*) can be estimated from network traffic, and we collect them in the (*wavelength*) load vector $\underline{u}=[u_1,\ldots,u_H]$.

Within a first-order perturbation analysis, the received SNR over the bandwidth of the DP signal of interest after propagation across the reference lightpath can be expressed as [13,14]

$$SNR(P,N_s,\underline{u})=\frac{P}{\beta(N_s+H)+a_{NL}(N_s,\underline{u})P^3} \tag{1}$$

where P is the DP reference signal power at the input of each transmission fiber section; $N_A\triangleq\beta(N_s+H)$ is the amplified spontaneous emission (ASE) power from the (N_s+H) optical amplifiers, with $\beta\triangleq h\nu FGB_r$, where h is Planck's constant, ν is the optical carrier frequency, F is the amplifier noise figure, G is the amplifier gain (equal to the span loss) and B_{rx} is the receiver equivalent noise bandwidth; a_{NL} is the nonlinear interference (NLI) coefficient [13,10] which depends on the number of spans and on the load vector $\underline{u}$, which in turn depends on the offered traffic and on the RWA algorithm. Since the number of interfering wavelengths is a random variable (RV), then also the a_{NL} coefficient and the received SNR are RVs, whose statistics depend on $\underline{u}$. SNR is deterministic only in the two limiting cases $\underline{u}=\underline{0}$ (no interfering wavelengths along our lightpath , i.e., single channel propagation) and $\underline{u}=\underline{1}$ (full load operation) where there is no random variability of the number of interfering lightpaths.

We assume the digital signal is coded with a forward error-correction (FEC) code whose SNR threshold (plus margin) for the signal modulation format is S_0. We declare an SB event when $SNR(P,N_s,\underline{u})<S_0$. The circuit is in that case routed via multiple lightpaths and requires OER at intermediate nodes. In this work we do not consider a possible change of modulation format and/or FEC, in response to an SB event.

3. Summary of results

We anticipate in this section our main results regarding both the load-aware reach and the OER savings. Numerical results are provided for the simplified case of: (i) identical spans across the network; (ii) WDM signals with same spectrum, thus power and bandwidth; (iii) ON/OFF independent traffic on all $W-1$ interfering wavelengths at each hop along the reference lightpath; and (iv) uniform load at all hops, i.e., $u_k\equiv u$ for all $k=1,\ldots,H$.

It should be clear that such assumptions are highly simplistic, and are justified only in view of a first coarse analysis of the possible gains of the proposed method. Extensions of the theory to hop-dependent loads, still assuming independent per-wavelength traffic, are presented in Section 4. In actual network operation, however, there will be clear dependencies between wavelengths used on one link and on the next link. There are also dependencies between wavelengths used on the same link, especially when impairment-aware RWA algorithms are used to allocate lightpaths. The theory of such correlations is partly tackled in the more advanced Markovian traffic model analyzed in Appendix B.

3.1. SNR blocking probability contours

The key ideas of our proposed load-aware regeneration strategy are best understood from the following discussion. The design of point-to-point DU transmission for high symbol rate DP WDM coherent systems is based on contours of the deterministic received SNR (for the worst-case reference channel of interest, normally the center WDM channel) versus both transmitted power P and number of spans N_s (see, e.g., [15]). An example of such deterministic SNR contours is given at $u=0$ and $u=1$ in Fig. 2: there we show the SNR contours at level $S_0=9.8$ dB for a point-to-point DP-QPSK WDM system (bit-error rate (BER) equal to 10^{-3} without differential decoding) over an $N_s\times 100$ km DU link with non-zero dispersion shifted fiber (NZDSF: dispersion $D=2$ ps/nm/km, attenuation $\alpha=0.2$ dB/km, $n_2=2.5\times 10^{-20}$ m^2/W, $A_{eff}=80$ μm^2 at $\lambda=1550$ nm) with either a

[1] Note that add/drop and switching are commonly performed at the same location. However, a hop in our treatment logically corresponds to a segment between add/drop nodes.

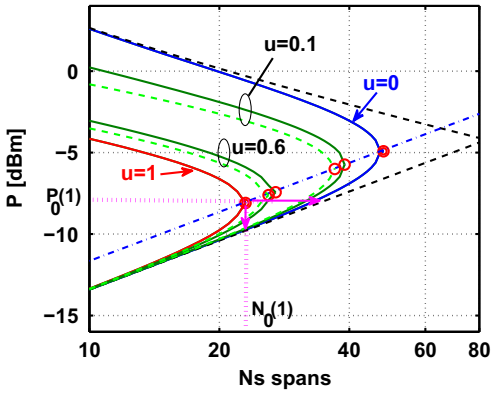

Fig. 2. (Curves at wavelength loads $u=0$ and $u=1$): Contours of center-channel SNR at level $S_0=9.8$ dB (BER $=10^{-3}$) versus power P and number of spans N_s for a point-to-point DP-QPSK WDM system over an $N_s\times 100$ km NZDSF DU link with either only our reference lightpath ($u=0$) or $W=81$ filled wavelengths ($u=1$). Symbol rate $R=10$ Gbaud. Spacing $\Delta f=12.5$ GHz. Amplifiers noise figure $F=4$ dB. Linear and nonlinear asymptotes shown as black dashed lines. Locus of maximum reach points shown as blue dashed-dotted line parallel to (lower) linear asymptote, upward shifted by 1.76 dB. (Curves at loads $u=0.1$ and $u=0.6$): contours of SNR-blocking probability at level $\mathcal{P}_{SB}$ versus P and N_s for the same link and $W=81$ wavelengths carrying ON/OFF traffic. All pairs (P,N_s) inside each contour yield $\Pr\{SNR(P,N_s,u)<S_0\}\le\mathcal{P}_{SB}$. Dashed contours at level $\mathcal{P}_{SB}=10^{-3}$, solid contours at level $\mathcal{P}_{SB}=0.5$. $\mathcal{S}=2$ span/hop. (For interpretation of the references to color in this figure, the reader is referred to the web version of this paper.)

single reference channel ($u=0$) or $W=81$ wavelengths all carrying DP-QPSK signals ($u=1$) . The symbol rate was $R=10$ Gbaud, the spacing $\Delta f=12.5$ GHz (spectral fill factor $\eta=\frac{R}{\Delta f}=0.8$), and the amplifiers noise figure $F=4$ dB. A value $\mathcal{S}=2$ span/hop was used in the calculations. No polarization-mode dispersion (PMD) was assumed in the line. Linear and nonlinear asymptotes are shown as black dashed lines. The optimal-power/maximum-reach points (red circles) fall on top of the blue dashed-dotted line parallel to the (lower) linear asymptote, upward shifted by 1.76 dB (see [15] and Appendix A). Rectangular signal spectra were used in the a_{NL} calculations according to our time-domain calculations [16] of the coherent GN model [10]. The system parameters were chosen to provide a large gap between single-channel and full load SNR contours in Fig. 2.

In a network scenario with a load value $0<u<1$, instead, the received SNR for the reference channel becomes a RV, since the number of interfering lightpaths, i.e., wavelengths that carry power along the reference signal's path, is a RV. Thus we cannot use the deterministic SNR contours anymore. What do we use then?

The scenario is reminiscent of a point-to-point link with PMD, or any non-ergodic process that turns the transmission channel into a stochastic channel. In such cases the SNR, which determines the BER, is not enough to fully describe performance, and the outage probability, i.e., the probability that BER or SNR exceed a prescribed threshold, must be provided as well. The "outage event" is in our network scenario the SB event. In this paper, for the first time, we propose to base the transmission design of DU networks on the *SNR* blocking probability

$$P_{SB}(P,N_s)\triangleq \mathrm{P}\{SNR(P,N_s,u)<S_0\} \tag{2}$$

at fixed wavelength load u and FEC threshold S_0. The design looks at the contour $P_{SB}(P,N_s)=\mathcal{P}_{SB}$ at a specified target SB probability level $\mathcal{P}_{SB}$ and load u, and seeks the point at maximum reach.

Examples of such contours are shown in Fig. 2 at loads $u=0.1$ and $u=0.6$ both at level $\mathcal{P}_{SB}=10^{-3}$ (dashed contours) and at level $\mathcal{P}_{SB}=0.5$ (solid contours). In our proposal, we assume the QoT-aware RWA has only knowledge of the wavelength load u and does not keep network-wide wavelength state tables: it thus ignores the exact state of each specific wavelength in the network, which justifies the SNR randomness assumption. Our RWA will decide that a new lightpath of length N_s spans has sufficient SNR at destination if P_{SB} is less than or equal to the target level $\mathcal{P}_{SB}$ for the selected lightpath modulation format. If such a decision is made, the lightpath is set up and kept active until an SB event is detected. Of course, our RWA decisions can be wrong with probability less than $\mathcal{P}_{SB}$, in which case the receiver will signal back to the transmitter RWA, and the lightpath will be segmented into more lightpaths.

From the P_{SB} contours versus P and N_s at the specified level $\mathcal{P}_{SB}$ and load u we can visualize both the maximum number of spans that can be bridged without OER, i.e., the load-dependent reach $N_0(u)$, and its associated optimal power $P_0(u)$.

In Fig. 2, the optimal-power/maximum-reach points $(P_0(u),N_0(u))$ at loads $u=0.1$ and $u=0.6$ are again marked by circles.

Note that at $u=1$ and $u=0$ the SB contours at all $\mathcal{P}_{SB}$ levels coincide with the $SNR=S_0$ contours, since for all (P,N_s) pairs inside such contours the SB probability is exactly zero, while outside it is exactly 1. Instead, at any other intermediate load $0<u<1$ the contours change with the value of $\mathcal{P}_{SB}$. However, we note that the dashed and solid contours at both $u=0.1$ and $u=0.6$ are quite close to each other, and it can be shown that they get closer and closer as the number of spans per hop $\mathcal{S}$ decreases. This is an indication that the transition of SB probability from zero to 1 is rather sharp. SB contours at practical levels will be close to the one at level $\mathcal{P}_{SB}=0.5$, which – as we shall prove in Section 4 – coincides with the following SNR contour at level S_0:

$$SNR(E[a_{NL}])\triangleq\frac{P}{\beta(N_s+H)+E[a_{NL}(N_s,u)]P^3}=S_0 \tag{3}$$

i.e., the classical *deterministic* SNR contour for point-to-point linkswhere the traffic-averaged coefficient $E[a_{NL}]$ is used in place of a_{NL}. For the SNR contour (3), we prove in Appendix A that its locus of maximum reach points, as $E[a_{NL}]$ varies, lays on the dashed-dotted straight line shown in Fig. 2 parallel to the (lower) linear asymptote and shifted by $10\log_{10}(3/2)\cong 1.76$ dB above that. In the log–log plot of Fig. 2 the linear asymptote and hence the dashed-dotted line have slope 1 dB/dB.

Please cite this article as: A. Bononi, et al., Regeneration savings in flexible optical networks with a new load-aware reach maximization, Optical Switching and Networking (2015), http://dx.doi.org/10.1016/j.osn.2015.07.003

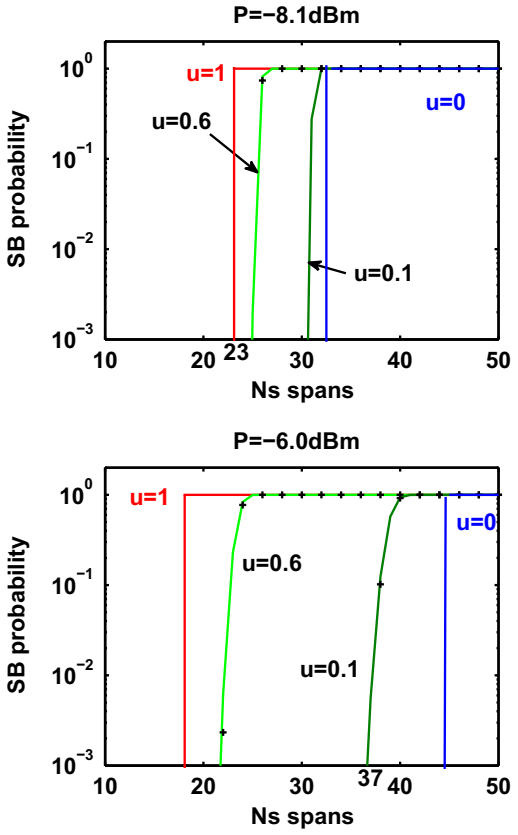

Fig. 3. "Vertical cuts" of the same SB probability surface whose contours ("horizontal cuts") are shown in Fig. 2, at the two fixed powers: $P_0(1) = -8.1$ dB (top) ; $P_0(0.1) = -6$ dB (bottom). Crosses indicate the exact outage probability obtained with the exact PDF for a_{NL}, solid lines use instead a Gaussian PDF fit for a_{NL} (see discussion of Fig. 11).

3.2. Reach under-estimation

By the above reasoning, the magenta arrows in Fig. 2 indicate 1.76 dB on each axis direction. This has a fundamental consequence, first noted in [6]. If we set P to the *full load* value $P_0(1)$ (shown in the figure) then the ratio between the full-load reach $N_0(1)$ and the maximum reach $N_0(u)$ at any other load $u < 1$ is always smaller than 2/3. Thus, if in the QoT-aware RWA algorithm we set the maximum non-regenerative reach to its full-load value $N_0(1)$, at most we under-estimate the true reach by a factor 1/3, i.e., by 33% [6]. This was the rationale for proposing a full-load QoT-aware RWA design using the distance-independent full load power $P_0(1)$ in [6].

To check the predictions in [6], we can slice the P_{SB} surface in Fig. 2 along the magenta dotted line at full-load optimal power $P \equiv P_0(1) = -8.1$ dBm. Fig. 3 (top) shows such a cut, namely P_{SB} versus N_s. At a level $P_{SB} = 10^{-3}$, we see that when we use power $P_0(1)$ at a load $u = 0.1$ the true reach is 30 spans, while the full-load reach is 23 spans, with an under-estimation with respect to the true reach by only $\frac{30-23}{30} \times 100 = 23.3\%$ which is below 33%, as forecast by [6]. However, when the actual load is $u = 0.1$, the maximum reach power is $P \equiv P_0(u) = -6$ dBm, and if we slice the P_{SB} surface in Fig. 2 at such a power we obtain the curves in Fig. 3 (bottom), where we note that the actual reach is $N_0(u) = 37$ spans, which compared with the full-load reach $N_0(1) = 23$ spans gives a transparent reach under-estimation by the full-load RWA with respect to the true reach by

$$\mathcal{U} \triangleq \frac{N_0(u) - N_0(1)}{N_0(u)} 100 = 37.8\% \tag{4}$$

which is above 33% in this example. This means that if we know the average wavelength load u and then select the optimal maximum reach power $P_0(u)$ (whose explicit formula is provided later in (27)), the reach under-estimation with respect to the true reach $N_0(u)$ when we use the full-load RWA can be larger than 33%.

By solving the implicit Eq. (26) of Section 4 we can directly obtain the maximum reach values $N_0(u)$ at any load u and the corresponding optimal power $P_0(u)$.

Fig. 4 (top) shows $N_0(u)$ and Fig. 4 (bottom) shows under-estimation $\mathcal{U}$ in (4), both plotted versus transmission fiber dispersion D at several load values. We note a diminishing under-estimation at both increasing dispersion and load, which is due to a diminishing impact of cross-channel nonlinearity. For standard single-mode fiber (SMF) with $D = 17$ ps/nm/km, and at a symbol rate $R = 10$ Gbaud, the under-estimation is below 33% at loads

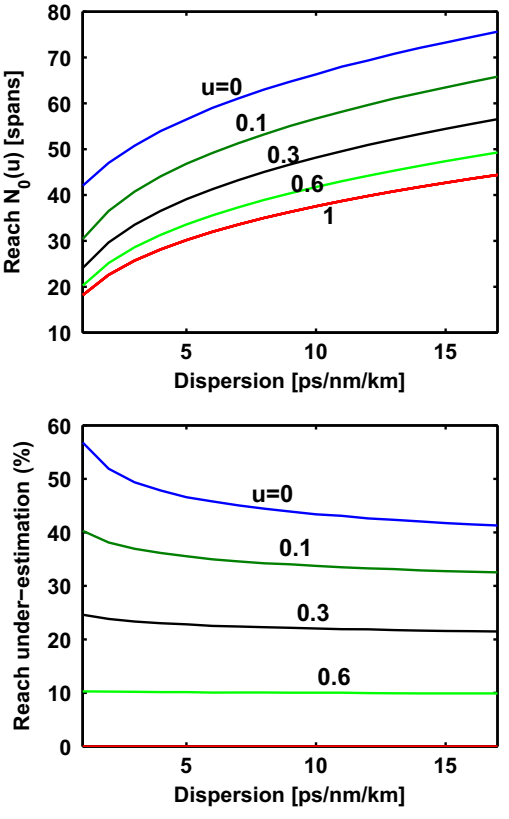

Fig. 4. (Top) maximum reach $N_0(u)$ of same SB probability contours at $\mathcal{P}_{SB} = 10^{-3}$ as in Fig. 2, versus transmission fiber dispersion D at several load values. (Bottom) Corresponding reach under-estimation $\mathcal{U}$ of full-load policy w.r.t. load-aware policy, Eq. (4). Data: $W = 81$, $R = 10$ Gbaud, $\Delta f = 12.5$ GHz, $\mathcal{S} = 2$, span length 100 km, $S_0 = 9.8$ dB, $F = 4$ dB, $\mathcal{P}_{SB} = 10^{-3}$. Dispersion axis starts at 2 ps/nm/km.

Please cite this article as: A. Bononi, et al., Regeneration savings in flexible optical networks with a new load-aware reach maximization, Optical Switching and Networking (2015), http://dx.doi.org/10.1016/j.osn.2015.07.003

$u \geq 0.1$. At loads above 0.3 there is essentially no dependence on dispersion.

Fig. 5 shows the reach under-estimation $\mathcal{U}$ versus load u for the same system parameters as in Fig. 2, except that transmission fiber is now SMF and we look at two symbol rates $R=10$ Gbaud and $R=28$ Gbaud (solid lines) while scaling frequency spacing as $\Delta f = R/\eta$, at fixed bandwidth efficiency $\eta = 0.8$. We note that reach under-estimation $\mathcal{U}$ quickly decreases with load u, and also decreases as we increase the channel symbol rate R at constant η, i.e., when single-channel nonlinear effects become more important [16, Fig. 6]. On SMF we see that $\mathcal{U}$ goes below 30% as soon as the load u exceeds 0.1. So on SMF, if we judge the goodness of the full-load regeneration strategy from the reach underestimation $\mathcal{U}$, we conclude that it makes sense at all practical loads.

We also considered the case of ideal digital back-propagation (DBP), when single-channel interference (SCI) is fully suppressed. DBP makes the gap of SNR contours between full load and zero load approach infinity, so we expect to be back to large-gap case exemplified by Fig. 2. However, we see that even with DBP, when the transmission fiber is SMF the reach underestimation of the full-load strategy is below 30% at all loads larger than 0.3.

Note that with ideal DBP only cross-nonlinear effects remain, and the reach N_0 is essentially independent of the channel symbol rate and just depends on bandwidth efficiency η [18]. Hence the dashed DBP curve in Fig. 5 is almost independent of symbol rate R.

3.3. Regeneration savings

If we had to judge the goodness of the standard full-load reach approach from its reach underestimation $\mathcal{U}$ with respect to the optimal load-aware reach, from the above results we would conclude that on SMF fiber the standard approach is always a good choice at any practical loads and symbol rates, even with DBP.

However, one fact should make us question the validity of the comparison parameter $\mathcal{U}$: for its evaluation the network topology did not play any role, and traffic was summarized by just the wavelength load.

We next provide another comparison parameter: the savings in OE regenerations when using either the full-load RWA or our load-aware reach-maximizing RWA. A quick approximate quantification is obtained as follows. We obtain the distribution of the lightpath length N_s (spans) in a selected network whose topology is fully specified, from detailed traffic simulations *when SNR blocking is neglected*. We start from an empty network, generate call requests according to the selected traffic matrix, and set up single-lightpath circuits (for all distances) for incoming requests until we hit the first WB, where we record the load u. Let the obtained normalized histogram of lightpath lengths N_s (i.e., the empirical probability mass function (PMF) of N_s) be $\mathcal{P}(N_s, u)$. Fig. 6 shows an instance of such a PMF at first WB from one simulation in a 46-node U.S. network (labeled US) [19] when the traffic matrix is uniform over the nodes and shortest path routing is selected. The measured network-averaged wavelength load was $u=0.46$. From such a PMF, we can estimate the expected number of required OE regenerations $\mathcal{N}_E$ when the reach is N_0 as

$$E[\mathcal{N}_E|N_0] = \sum_{N_s=1}^{N_{max}} \mathcal{P}(N_s,u)\left(\lceil \frac{N_s}{N_0} \rceil - 1\right) \tag{5}$$

where N_{max} is the maximal N_s in the network, and $\lceil x \rceil$ is the ceiling function. The *percent savings* $\mathcal{R}(u)$ in OER operations using our load-aware RWA with respect to the full-load RWA is

$$\mathcal{R}(u) = \frac{E[\mathcal{N}_E|N_0(1)] - E[\mathcal{N}_E|N_0(u)]}{E[\mathcal{N}_E|N_0(1)]} \cdot 100. \tag{6}$$

Note that whenever $N_0(1) < N_{max} < N_0(u)$ the savings are 100% since no regenerations are required with the load-aware RWA. Fig. 7 shows both the underestimation $\mathcal{U}$, Eq. (4), and the savings $\mathcal{R}(u)$, Eq. (6), versus load u at first WB for both the U.S. network and a 20-node European (EU) network [20], for a W=89 wavelength WDM DP-QPSK system at $R=28$ Gbaud and spacing $\Delta f = 35$ GHz over SMF fiber. The remaining parameters for the calculation of $N_0(1)$ and $N_0(u)$ in (6) are as in Fig. 2. In particular, $\mathcal{S}=2$ spans/hop were assumed, although the EU and U.S. topologies had an average of 7.1 and 5.3 spans between

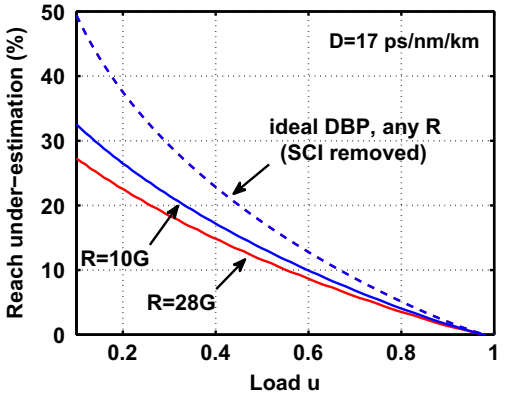

Fig. 5. Reach under-estimation $\mathcal{U}$, Eq. (4), versus load u in a DU SMF link ($D=17$ ps/nm/km) with $W=81$ WDM DP-QPSK channels at R Gbaud/channel and constant bandwidth efficiency $\eta = \frac{R}{\Delta f} = 0.8$, at SNR blocking probability $\mathcal{P}_{SB} = 10^{-3}$. Other data as in Fig. 2.

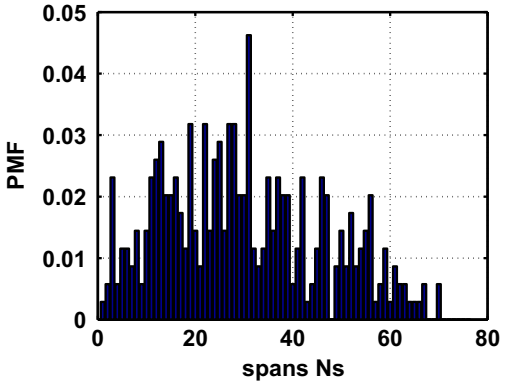

Fig. 6. Normalized histogram of lightpath lengths (spans) obtained from one path-setup simulation in a 46-node U.S. network at first wavelength blocking. Measured load was $u=0.46$, with a total of 346 lightpaths at WB.

Please cite this article as: A. Bononi, et al., Regeneration savings in flexible optical networks with a new load-aware reach maximization, Optical Switching and Networking (2015), http://dx.doi.org/10.1016/j.osn.2015.07.003

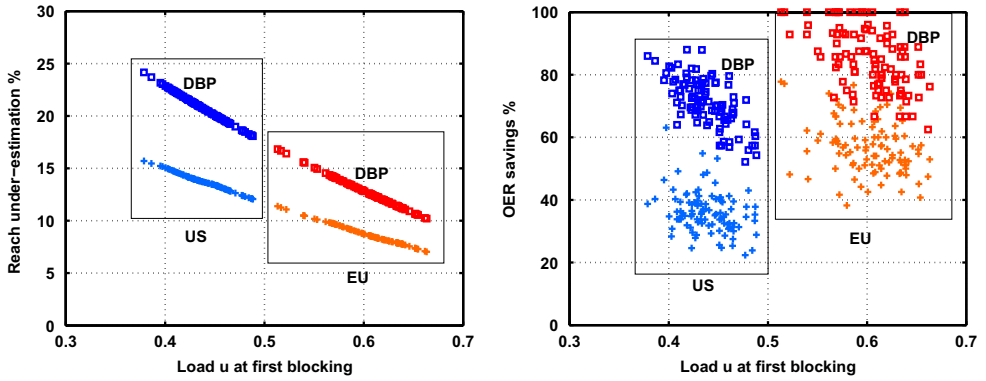

Fig. 7. (Left) Underestimation $\mathcal{U}$ (4) and (Right) regenerations savings $\mathcal{R}$ (6) vs load u at first wavelength blocking in the U.S. and European (EU) networks for a W=89 wavelengths WDM DP-QPSK system at $R=$ 28 Gbaud and $\eta=\frac{R}{\Delta f}=0.8$ over SMF fiber ($D=17$ ps/nm/km). Remaining parameters as in Fig. 2. Squares: DBP. Crosses: without DBP.

switching nodes (hence we assumed that traffic can enter/exit also at about two intermediate places along a link from switching node to switching node). Also, a uniform value $u_k=u$ coinciding with the network average at first wavelength blocking was used to get $N_0(u)$ from the implicit Eq. (26). The results of 100 different runs are reported in the figures. Squares are for ideal DBP, crosses are without DBP. OER savings of more than 20% and 38% are obtained in the U.S. and EU networks, respectively. Using single-channel nonlinearity suppression with an ideal DBP increases the savings to more than 50% in the US and 60% in the EU networks, respectively. The important message is that reach under-estimation $\mathcal{U}$ may not be a good indicator of OER savings. Even at relatively small under-estimations as in the EU network, the savings in OER with respect to the standard full-load choice $N_0(1)$ can be significant. The reason is that $\mathcal{R}(u)$ depends both on the difference $N_0(u)-N_0(1)$ and on how quickly the PMF decreases to zero beyond $N_0(1)$.

We finally check the effect of the modulation-dependent target SNR S_0 on OER savings. Fig. 8 shows OER savings $\mathcal{R}$ (red) and under-estimation $\mathcal{U}$ (blue) versus S_0 at the first WB load $u=0.46$ in the U.S. network in uniform traffic, at $R=28$ Gbaud on SMF fiber, both with (solid) and without (dashed) ideal DBP. We note that at the smallest S_0 of 6.8 dB (e.g., corresponding to DP binary phase shift keying at BER$=10^{-3}$) no regenerations are needed in the network even using $N_0(1)$, hence $\mathcal{R}$ is undefined. As we increase S_0 we go to a situation where $N_0(1)<N_{max}<N_0(u)$, yielding 100% savings. As the number of modulation levels increases, the required S_0 increases as well (e.g., $S_0=16.5$ dB for DP 16 quadrature-amplitude modulation), hence N_0 decreases, and the % OER savings $\mathcal{R}$ decrease towards the values of under-estimation $\mathcal{U}$. Thus under-estimation is also a reasonable indicator of % OER savings only for higher-order modulation formats in this example.

4. Details of reach analysis

While the objective of the previous section was to provide a coarse quantification of the potential gain in maximum reach and OER savings of our load-aware RWA design with respect to the standard full-load RWA, this section will provide all the theoretical details necessary to explain the presented numerical results, and extend the theory by relaxing some of the stringent assumptions of the previous numerical results section.

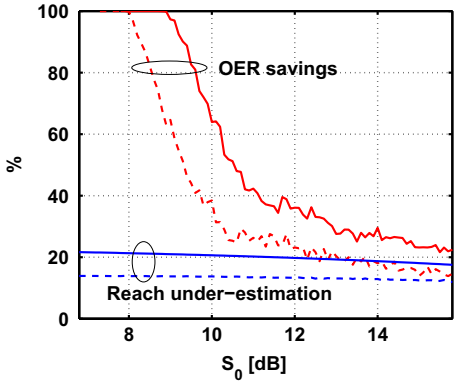

Fig. 8. OER savings $\mathcal{R}$ (red) and under-estimation $\mathcal{U}$ (blue) versus target SNR S_0 (i.e., modulation format) at the first-WB in the U.S. network [19], at $R=28$ Gbaud on SMF fiber. Other data as in Fig. 2. Solid: ideal DBP. Dashed: no DBP. $\mathcal{R}$ and $\mathcal{U}$ averaged over 100 simulations up to first WB; average load $u=0.46$. (For interpretation of the references to color in this figure caption, the reader is referred to the web version of this paper.)

4.1. Nonlinear interference coefficient

Fig. 9 sketches a link from source node S to destination node D for a reference lightpath at wavelength λ_{ref}. The number of hops is H, and generic hop k is composed of $\mathcal{S}_k$ spans. Traffic on the reference lightpath enters at S and exits at D. On all other wavelengths, traffic may exit at any intermediate node, then re-enter at a later node (with different data), then exit, and so forth. Each thick line with ending arrow indicates a lightpath. We define

$u_k=\Pr\{\text{a wavelength is carrying a lightpath at hop } k\}$.

This quantity can be estimated as the long-run average number of active lightpaths at hop k, divided by the total number of per-fiber wavelengths W. The load vector

Please cite this article as: A. Bononi, et al., Regeneration savings in flexible optical networks with a new load-aware reach maximization, Optical Switching and Networking (2015), http://dx.doi.org/10.1016/j.osn.2015.07.003

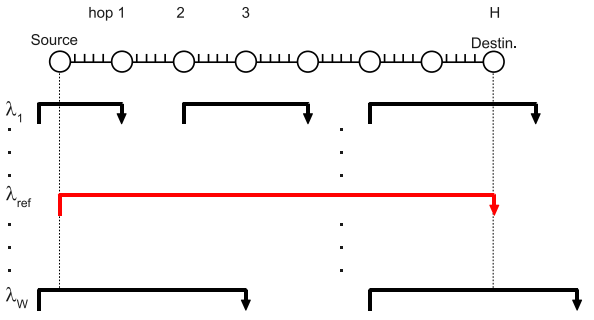

Fig. 9. Example of link crossed by reference lightpath at λ_{ref} from Source to Destination node, with $H=7$ hops and $\mathcal{S}=5$ spans per hop. Interfering lightpaths on wavelengths λ_1 through λ_W may enter/exit at any node.

$\underline{u}=[u_1,\ldots,u_H]$ is the only "traffic parameter" available to the RWA block.

In DU networks, or more generally in networks with large-enough residual dispersion per span such that the coherent GN model [10] applies, the received SNR of the DP reference signal when all WDM interferers propagate along the S-D path together with the reference signal is given by Eq. (1), where the NLI power $P_{NLI}=a_{NL}P^3$ is [10–12,16]:

$$P_{NLI}=B_{rx}\frac{16}{27}\int\int|\mathcal{K}(f_1f_2)|^2G(f_1)G(f_2)G(f_1+f_2)\,df_1\,df_2 \tag{7}$$

where B_{rx} is the noise equivalent bandwidth of the receiver, $G(f)$ is the power spectral density (PSD) of the DP WDM comb, and $\mathcal{K}(v)$ is the (un-normalized) link kernel from node S at coordinate $z=0$ to node D at coordinate $z=L$, with $v=f_1\cdot f_2$, whose expression in absence of dispersion slope is [11,12,17]

$$\mathcal{K}(v)=\int_0^L\gamma(z)\mathcal{G}(z)e^{-j\frac{(2\pi)^2v}{2}C(z)}dz \tag{8}$$

with γ the nonlinear fiber coefficient, $\mathcal{G}(z)=P(z)/P(0)$ the power gain from 0 to $z\in[0,L]$, and $C(z)=-\int_0^z\beta_2(s)ds$ the cumulated chromatic dispersion from 0 to z. We assume that link gain/loss and total dispersion are perfectly compensated for at the coherent receiver.

Assuming channels have a rectangular spectrum, Fig. 10 shows as colored "islands" the integration domain of the double frequency integral in (7) [10,16]. If any of the WDM signals is switched off, we have to switch off its corresponding PSD and thus remove the corresponding islands (e.g. when removing channel 2, those islands colored in blue in the figure). Fig. 10 shows one contour level of the function $|\mathcal{K}(f_1f_2)|^2$ (green dashed). Such contours are hyperbolas, as they just depend on the product $v=f_1\cdot f_2$. The central island accounts for the single channel interference. The remaining islands along the axes account for cross-channel interference (XCI), which also includes polarization-dependent effects. Off-axes islands account for four-wave mixing (FWM) among channels. FWM is normally negligible in DU links [10]. Neglecting FWM, the NLI coefficient can be written as

$$a_{NL}=a_{SCI}+a_{XCI} \tag{9}$$

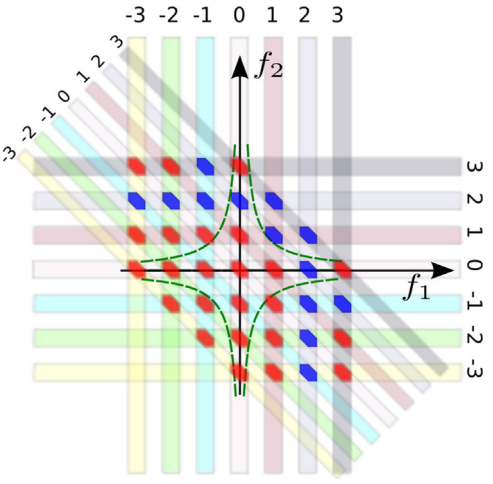

Fig. 10. Example of double integration domain (red and blue "islands") in (7) when spectra are rectangular with uniform channel spacing. Vertical stripes correspond to $G(f_1)$, horizontal stripes to $G(f_2)$, and 45° tilted stripes to $G(f_1+f_2)$. When switching a channel OFF (e.g. channel 2) the corresponding PSD is zeroed, and so are the corresponding islands (blue "islands"). (For interpretation of the references to color in this figure caption, the reader is referred to the web version of this paper.)

and in [16] we found that with rectangular spectra the SCI coefficient in the coherent GN model may be well approximated at large enough symbol rate/dispersion as

$$a_{SCI}\cong\frac{16}{27}\frac{B_{rx}}{B_0}\left[\frac{4}{B_0^2}\int_0^{(B_0/2)^2}|\mathcal{K}(v)|^2\log\left(\frac{(B_0/2)^2}{v}\right)dv\right] \tag{10}$$

where B_0 is the reference signal one-sided equivalent nonlinear optical bandwidth. It corresponds to integration of (7) over a square of edge B_0 centered at the origin [10]. In the numerical calculations in Section 3 we assumed $B_0\equiv k_{NL}R$ and $B_{rx}=k_LR$, where k_L is found by bit-error rate (BER) matching with simulations in the linear regime. Once k_L is fixed, then k_{NL} is found by matching with simulated SNR contours. The values we found to best match our simulations were $k_L=1$ (i.e., ideal matched filtering – a normal situation in presence of a linear equalizer) and $k_{NL}=1.25$.

When all pumps propagate together with the signal, by generalizing the coherent GN model calculations with rectangular signal spectra in [16, Eq. (20)],[2] we find that the dual-polarization XCI NLI coefficient can be tightly upper-bounded at large-enough channel spacing times symbol rate product $\Delta f\cdot R$ as

$$a_{XCI}=\frac{16}{27}\frac{B_{rx}}{B_0}\int_0^\infty\left|\mathcal{K}(v)\right|^2dv\sum_{p\neq0}g_p \tag{11}$$

where the sum is extended to all interfering *pumps* p (or lightpaths) distinct from the reference lightpath with

[2] A typo is present in [16, Eq. (20)]: a "ln" is missing in front of the square bracket.

Please cite this article as: A. Bononi, et al., Regeneration savings in flexible optical networks with a new load-aware reach maximization, Optical Switching and Networking (2015), http://dx.doi.org/10.1016/j.osn.2015.07.003

index 0, and

$$g_p \triangleq \frac{4}{B_p}\left(\frac{P_p}{P}\right)^2 \ln\left(\frac{1+\frac{B_p}{2\Delta f_p}}{1-\frac{B_p}{2\Delta f_p}}\right) \tag{12}$$

where (P_p, B_p) are the p-th pump optical power and bandwidth (P is the power of the reference channel), and $\Delta f_p = |f_p - f_0|$ is the carrier frequency offset of pump p from the reference lightpath. The above formula can handle point-to-point links with unequal spans and WDM transmissions with flexible spectrum/format allocation. The same analytical approximation for the XCI contribution was independently derived by using the incoherent GN model in [7, Eq. (16)] for the special case of identical lossy spans with end-span lumped amplification.

By using [16, Appendix B], we easily find that for links without end-hop dispersion compensation (e.g. DU links, but here we also allow for dispersion management within a hop) we exactly have

$$\int_0^\infty |\mathcal{K}(\nu)|^2\, d\nu = \sum_{k=1}^{H} \int_0^\infty |\mathcal{K}_k(\nu)|^2\, d\nu \tag{13}$$

where the hop-h kernel is

$$\mathcal{K}_k(\nu) = \int_{z_{i,k}}^{z_{o,k}} \gamma(z)\mathcal{G}(z) e^{-j(2\pi)^2\nu/2)\mathcal{C}(z)}\, dz \tag{14}$$

with $(z_{i,k}, z_{o,k})$ the input/output coordinates of hop k. Eq. (13) physically means that the XCI contributions of the various hops are completely uncorrelated.

In the classical coherent GN model treatment [10,11,16,17] that leads to Eqs. (11)–(14), all WDM channels enter at the same node S and exit at the same node D, hence the kernel seen by the pumps is the same as the kernel seen by the reference channel (13). However, we now allow the non-overlapping lightpaths on λ_p (there may be more than one, as shown in Fig. 9) to enter and exit at arbitrary nodes along the route from S to D, and to possibly carry different modulation formats. Define the wavelength occupancy indicator $I_{pk} = 1$ if a lightpath is present on λ_p at hop k, and $I_{pk} = 0$ otherwise. Thus for links without end-hop dispersion compensation, Eq. (11) generalizes to

$$a_{XCI} = \mathcal{C}_0 \sum_{p\neq 0} \sum_{k=1}^{H} \mathcal{I}_k I_{pk} g_{pk} \tag{15}$$

where g_{pk} is defined in (12) and uses hop-dependent power and bandwidth (P_{pk}, B_{pk}), and we defined

$$\mathcal{C}_0 \triangleq \frac{16}{27}\frac{B_{rx}}{B_0} \tag{16}$$

$$\mathcal{I}_k \triangleq \int_0^\infty |\mathcal{K}_k(\nu)|^2\, d\nu. \tag{17}$$

The mean $\eta_a \triangleq E[a_{XCI}]$ and the variance $\sigma_a^2 \triangleq Var[a_{XCI}]$ are easily calculated from (15) when (i) the RVs $\{I_{pk}\}$ are independent for all p and k, with known mean $E[I_{pk}] = u_k$ equal for all wavelengths at hop k; (ii) the modulation-dependent RV's $\{g_{pk}\}$ are independent for all p and k, and independent of the load variables $\{I_{pk}\}$, with known mean $E[g_{pk}] = \eta_{g,p}$ and variance $Var[g_{pk}] = \sigma_{g,p}^2$, equal for all hops on λ_p. This produces an independent ON/OFF traffic model on each wavelength. An alternative Markovian traffic model that accounts for correlations of wavelengths from hop to hop is presented in Appendix B. For the ON/OFF independent traffic we find from (15) that

$$\eta_a = \mathcal{C}_0 \sum_{p\neq 0} \eta_{g,p} \sum_{k=1}^{H} \mathcal{I}_k u_k \tag{18}$$

$$\sigma_a^2 = \mathcal{C}_0^2 \sum_{p\neq 0} \sum_{k=1}^{H} \mathcal{I}_k^2 [(\eta_{g,p}^2 + \sigma_{g,p}^2)u_k - \eta_{g,p}^2 u_k^2] \tag{19}$$

since $Var[g_{pk}I_{pk}] = E[g_{pk}^2]E[I_{pk}^2] - E^2[g_{pk}]E^2[I_{pk}]$.

In the numerical results in Section 3 we always used:

(i) identical spans and hops in the network, so that by again using [16, Appendix B], we get $\mathcal{I}_k = \mathcal{S}\mathcal{I}^{(1)}$, where $\mathcal{S}$ is the number of spans composing any hop k, and $\mathcal{I}^{(1)}$ is the single-span squared kernel integral;
(ii) the same spectrum for all signals, i.e., for all pumps we let $P_p = P, B_p = B_0$, and $\Delta f_p = |p|\Delta f$, with Δf the minimum channel spacing;
(iii) the ON/OFF traffic model in which $\sigma_{g,p}^2 = 0$;
(iv) a single load value $u_k \equiv u$ identical at all hops k.

4.2. SB contours

The a_{XCI} threshold value Θ that makes the received SNR equal to the FEC threshold, $SNR = S_0$, is obtained from (1) and (9) by solving the equation

$$S_0 = \frac{P}{\beta(N_s+H) + (a_{SCI}(N_s) + \Theta)P^3}. \tag{20}$$

Its explicit value is

$$\Theta(P, N_s) = \frac{1}{S_0 P^2} - \frac{\beta(N_s+H)}{P^3} - a_{SCI}(N_s) \tag{21}$$

and depends both on power P and on span index N_s. Since the SNR blocking event is $\{SNR < S_0\} = \{a_{XCI} > \Theta\}$, then the SB probability is computed as

$$P_{SB} \triangleq \mathrm{P}\{SNR < S_0\} = 1 - F_a(\Theta) \tag{22}$$

where $F_a(x) \triangleq \mathrm{P}\{a_{XCI} \le x\}$ is the cumulative distribution function (CDF) of the RV a_{XCI}. At level $P_{SB} = \mathcal{P}_{SB}$, the threshold Θ can then be obtained from the inverse CDF as $\Theta = F_a^{-1}(1-\mathcal{P}_{SB})$. By plugging back into (20), we obtain the SB contour at level $\mathcal{P}_{SB}$ as the solution of the following cubic equation in P:

$$P^3\left[a_{SCI} + F_a^{-1}(1-\mathcal{P}_{SB})\right] - \frac{P}{S_0} + \beta(N_s+H) = 0.$$

Its explicit Cardan's solutions (contour's upper branch P_M and lower branch P_m) are found explicitly as [15]

$$P_M = 3S_0\hat{N}_A \cos\left(\frac{\operatorname{acos}(-\beta(N_s+H)/\hat{N}_A)}{3}\right) \tag{23}$$

$$P_m = 3S_0\hat{N}_A \cos\left(\frac{2\pi - \operatorname{acos}(-\beta(N_s+H)/\hat{N}_A)}{3}\right) \tag{24}$$

Please cite this article as: A. Bononi, et al., Regeneration savings in flexible optical networks with a new load-aware reach maximization, Optical Switching and Networking (2015), http://dx.doi.org/10.1016/j.osn.2015.07.003

where the quantity

$$\hat{N}_A = \frac{2}{(3S_0)^{3/2}\sqrt{a_{SCI}(N_s)+F_a^{-1}(1-\mathcal{P}_{SB})}} \tag{25}$$

can be physically interpreted as the limit ASE power at which the top and bottom contour branches merge (when the acos(·) argument equals -1 we get $P_M = P_m$ from (23) and (24)). Hence the maximum number of spans N_0 at SB level $\mathcal{P}_{SB}$ can be obtained by numerically solving the implicit equation

$$\beta(N_0(\underline{u})+H) = \frac{2}{(3S_0)^{3/2}\sqrt{a_{SCI}(N_0)+F_a^{-1}(1-\mathcal{P}_{SB},\underline{u},N_0)}} \tag{26}$$

where we stressed in the notation that the threshold $\Theta = F_a^{-1}(1-\mathcal{P}_{SB})$ is also a function of both the load vector $\underline{u}$ and the maximum number of spans N_0. The corresponding max-reach power is finally obtained from (23)

$$P_0(\underline{u}) = \tfrac{3}{2}S_0\beta(N_0(\underline{u})+H). \tag{27}$$

The load-aware RWA algorithm solves Eqs. (26) and (27) in order to find the reach $N_0(\underline{u})$ and select/modify the power $P_0(\underline{u})$ of established lightpaths.

Although in principle the exact CDF F_a of a_{XCI} may be estimated from Monte-Carlo simulations of (15), a simple approximation is found as follows. Since the number of WDM wavelengths is normally large, it is clear from (15) that the RV a_{XCI} will be the sum of many independent random variables. By invoking the central limit theorem we may thus approximate a_{XCI} as a Gaussian RV, so that the SB probability "surface" (22) can be approximated as

$$P_{SB}(P,N_s) = 1-F_a(\Theta) \cong \mathcal{Q}\left(\frac{\Theta(P,N_s)-\eta_a(\underline{u},N_s)}{\sigma_a(\underline{u},N_s)}\right) \tag{28}$$

where $\mathcal{Q}(x) \triangleq \int_x^\infty \frac{1}{\sqrt{2\pi}}\exp\{-s^2/2\}\,ds$. Hence P_{SB} approximately just depends on a_{XCI} mean and variance (18) and (19).

For instance, consider the same network data used to obtain Fig. 3(top), where all hops have the same load u. Fig. 11 shows in dashed red the Gaussian probability density function (PDF) fit at loads $u=0.1$ and $u=0.6$ at $N_s=30$ spans. The threshold Θ, Eq. (21), is load-independent (it becomes load-dependent only when we impose a specific contour level $P_{SB}=\mathcal{P}_{SB}$) and is shown as a blue vertical line. As we increase the load u from zero the Gaussian PDF shifts towards the threshold (i.e. η_a increases). It broadens (σ_a increases) up to $u=0.5$ when variance reaches its maximum; variance then starts decreasing back to zero as we move towards full load $u=1$.

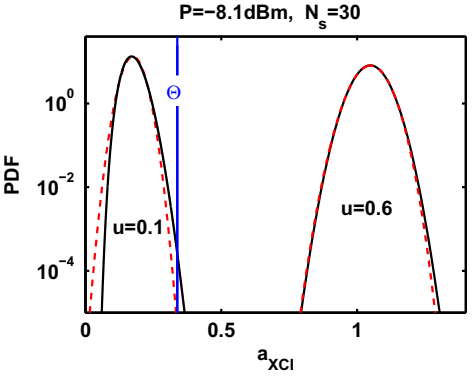

Fig. 11. (Left) Exact PDF for a_{XCI} (black solid) and fitted Gaussian PDF (red dashed) taken at $N_s=30$ spans (15 hops) and two load values $u=0.1$ and $u=0.6$, for the same example depicted in Fig. 3(top). Threshold value Θ shown as a vertical blue line. (For interpretation of the references to color in this figure caption, the reader is referred to the web version of this paper.)

The exact PDF obtained by Monte-Carlo simulations of (15) at $u=0.1$ and $u=0.6$ is reported in solid black. The Gaussian fit is seen to be quite reasonable, although the skewness of the exact PDF is such that the Gaussian fit tends to slightly under-estimate the SB probability.

By inverting (28) we get

$$\Theta = F_a^{-1}(1-\mathcal{P}_{SB}) \cong \mathcal{Q}^{-1}(\mathcal{P}_{SB})\sigma_a(\underline{u},N_s)+\eta_a(\underline{u},N_s) \tag{29}$$

where $\mathcal{Q}^{-1}$ is the inverse of $\mathcal{Q}(x)$. Eq. (29) is used to simplify Eqs. (26) and (27), which can thus be computed in real-time by the RWA unit.

Finally, please note that at $\mathcal{P}_{SB}=1/2$ we have $\mathcal{Q}^{-1}(\mathcal{P}_{SB})=0$, hence from (29): $\Theta=\eta_a\equiv E[a_{XCI}]$, and thus $a_{SCI}+\Theta = E[a_{SCI}+a_{XCI}] \equiv E[a_{NL}]$. Thus the (23) and (24) contour at $\mathcal{P}_{SB}=1/2$ coincides with the contour of the SNR (3) calculated with the expected value $E[a_{NL}]$ of a_{NL}.

5. Conclusions

This paper introduced a simple ON/OFF interfering WDM traffic model for flexible optical networks. The model summarizes the impact of the network traffic into a unique parameter, the wavelength load u. A key implication is that the stochastic behavior of the network is simply accounted for, so that new design rules can be applied. We derived the statistics of the stochastic received SNR and thus the SNR blocking probability. From it, we derived analytical expressions of the load-dependent maximum reach $N_0(u)$ and its corresponding optimal power $P_0(u)$ within the framework of the coherent GN model. Extensions to a traffic model with hop-by-hop correlations are also provided in Appendix B. A novel load-aware RWA algorithm was then proposed that uses the load-dependent reach $N_0(u)$ instead of the commonly used full-load reach $N_0(1)$. For such a novel load-aware RWA we quantified the possible savings in opto-electronic regenerations for two sample optical network topologies at the first wavelength blocking. For 28 Gbaud WDM DP-QPSK signals at 80% bandwidth efficiency over SMF DU transmissions with 100 km span length, average regenerations savings of more than 20% and 38% are obtained in America- and Europe-like networks, respectively, at the load corresponding to the first wavelength blocking. When single-channel nonlinearity is removed by an ideal DBP, the savings increase to more than 50% in the American and 60% in the European network, respectively.

This paper just scratched the surface regarding the possibility of moving towards flexible optical networks that more effectively exploit their hardware resources. We performed preliminary calculations aimed at roughly assessing how much can be saved in regenerations if the "play-it-safe" full-load reach paradigm is replaced with a more aggressive load-dependent reach paradigm.

Please cite this article as: A. Bononi, et al., Regeneration savings in flexible optical networks with a new load-aware reach maximization, Optical Switching and Networking (2015), http://dx.doi.org/10.1016/j.osn.2015.07.003

Our proposed new RWA algorithm does not need to keep network-wide wavelength state tables, and does make *statistical* decisions on whether to set-up a new lightpath or regenerate an existing one, based only on average wavelength load measurements.

In a static traffic scenario, where from a green field network the operator adds more and more lightpaths till the maximum possible load, the proposed load-aware method indicates a pay-as-you-go regenerators deployment strategy, so that capital expenditure need not be entirely payed upfront.

The price to pay is a continuous monitoring of the QoT of each wavelength so that, if the wavelength load increases and the estimated SNR blocking probability moves too close to the prescribed limit, then an intermediate regeneration will need to be introduced with live traffic at some node along the lightpath.

In a dynamic traffic scenario this may imply a significant computational burden on the RWA block. However, in such a dynamic traffic scenario it is already the wavelength fragmentation that poses serious wavelength load limits to flexible networks that have scarce wavelength conversion capabilities [21].

The introduction of extra wavelength conversion capabilities at add/drop nodes to reduce fragmentation will increase the network-wide wavelength utilization, and thus diminish the advantages of the proposed load-aware strategy.

Appendix A. Points at maximum reach

Consider the generic contour (3), such as the red, blue, and dark green contours in Fig. 2. Let N_0 be the maximum number of reachable spans and P_0 the corresponding power. Then the point (P_0, N_0) is the top of the bell curve (SNR versus power P) at distance N_0 when the top SNR value is S_0 [15]. But at the top of the bell curve, the ASE power $N_A = \beta(N_0 + H)$ is twice the NLI power [13], hence the SNR is $S_0 = \frac{P_0}{N_A + N_{NLI}} = \frac{P_0}{\frac{3}{2}\beta(N_0+H)}$ i.e., $P_0 = \frac{3}{2} S_0 \beta (N_0 + H)$ which is a straight line in the (P, N) plane, shifted by $(\frac{3}{2})^{\mathrm{dB}} \cong 1.76$ dB above the lower linear asymptote $P_0 = S_0\beta(N_0 + H)$. Such a line is the locus described by the coordinates of maximum reach as the NLI power (hence ASE, which has twice that power) is swept at constant β (i.e., constant amplifiers noise figure F).

Appendix B. Markov traffic model

Eq. (15) describes the a_{XCI} coefficient in DU networks. Its mean and variance were derived in (18) and (19) in the assumption of hop-independent ON/OFF traffic, where the modulation format of the interferers on any wavelength my change independently from hop to hop. This ON/OFF process does not capture hop-by-hop correlations. In this Appendix, we introduce a Markov traffic model that provides a more realistic description of the correlated traffic on each wavelength. For such a Markov traffic, we will derive the mean and variance, to be used in a Gaussian fit of the a_{XCI} PDF, as per Eq. (29).

In order to keep the treatment simple, we will assume here that all hops have identical spans, so that (17) yields $\mathcal{I}_k = \mathcal{S}_k \mathcal{I}^{(1)}$, where $\mathcal{S}_k$ is the number of spans composing hop k, and $\mathcal{I}^{(1)}$ is the single-span squared kernel integral. Then (15) becomes

$$a_{XCI} = \mathcal{C}_0 \mathcal{I}^{(1)} \sum_{p \neq 0} \left[\sum_{k=1}^{H} g_{pk} I_{pk} \mathcal{S}_k \right]. \tag{B.1}$$

Suppose a wavelength λ_p at a generic hop can be either idle (format 0) or carry one of F signal formats $m = 1, \ldots, F$. Hence define the process $X_{pk} = \{$ modulation format at hop k on $\lambda_p\} \in \{0, 1, \ldots, F\}$. Also, further classify the indicators I_{pk} in (B.1) according to their modulation format by introducing the indicators

$$I_{pk}(m) \triangleq \begin{cases} 1 & \text{if } X_{pk} = m \\ 0 & \text{else} \end{cases}$$

for all p, all $m \in \{0, 1, \ldots, F\}$, and $k \in [1, \ldots, H]$. Then the sojourn (in spans) in format m can be expressed as

$$N_{pm} = \sum_{k=1}^{H} I_{pk}(m) \mathcal{S}_k \quad [\text{spans}]. \tag{B.2}$$

By regrouping the contributions in (B.1) according to the signal format we get

$$a_{XCI} = \mathcal{C} \sum_{p \neq 0} \left[\sum_{m=1}^{F} g_{pm} N_{pm} \right] \tag{B.3}$$

where $\mathcal{C} \triangleq \mathcal{C}_0 \mathcal{I}^{(1)}$, and g_{pm} is defined in (12) and uses the known power and bandwidth (P_{pm}, B_{pm}) of signal format m at center frequency f_p.

Now, since $\{N_{pm}\}_{m=1}^{F}$ are correlated RVs, we must specify their joint distribution to find the distribution of the RV a_{XCI}. Our objective here is to just find its mean $\eta_a = E[a_{XCI}]$ and variance $\sigma_a^2 = Var[a_{XCI}]$.

We assume the traffic is independent on all wavelengths. Hence we focus on the occupancy of a single generic wavelength λ_p from hop 1 through hop H of the route selected for our new lightpath. We will thus omit the wavelength subscript p in all variables. We know the probability u_k that the wavelength is occupied at each hop k, for all $k = 1, \ldots, H$.

We now assume the process $\{X_k,\ k = 1, .., H\}$ on the generic wavelength is a non-homogeneous Markov chain, with ordered states $\{0, 1, \ldots, F\}$, characterized by the following probabilities:

(1) $\{P_m\}_{m=1}^{F}$: this is the a-priori PMF of signal formats in the network, hence $\sum_{m=1}^{F} P_m = 1$. This PMF can be estimated by taking the fraction of each format in a long-run simulation of the network at the load of interest.

(2) $\{\alpha_m\}_{m=1}^{F}$, where $\alpha_m =$ P {a lightpath with modulation format m which was active at the previous hop will remain active at the next hop}.

Then, the entries $p_{ij}(k) \triangleq \mathrm{P}\{X_k = i | X_{k-1} = j\}$ of the transition matrix $\mathbf{P}(k) = \{p_{ij}(k)\}_{i,j=0}^{F}$ at hop k are obtained (for

Please cite this article as: A. Bononi, et al., Regeneration savings in flexible optical networks with a new load-aware reach maximization, Optical Switching and Networking (2015), http://dx.doi.org/10.1016/j.osn.2015.07.003

$j \neq 0$) as

$$p_{ij}(k) = \begin{cases} 1-u_k & \text{if } i=0 \\ u_k \alpha_j & \text{if } i=j \\ u_k(1-\alpha_j)\dfrac{P_i}{1-P_j} & \text{else} \end{cases}$$

In words: if at hop $k-1$ the non-empty modulation format was j, then at hop k the new format will be the empty one with probability $1-u_k$. If not (with probability u_k), then with probability α_j X_k will remain on the same format as at hop $k-1$, or change format with probability $1-\alpha_j$. If a change occurs from the format j used at hop $k-1$, it will be towards all non-empty formats (excluding the j-th) according to the conditional PMF $\left\{\frac{P_i}{1-P_j}, i=1,\ldots,F,\ i\neq j\right\}$.

For $j=0$ we have instead

$$p_{i0}(k) \triangleq \mathrm{P}\{X_k = i | X_{k-1}=0\} = \begin{cases} 1-u_k & \text{if } i=0 \\ u_k P_i & \text{if } i\neq 0. \end{cases}$$

We therefore have complete knowledge of the H chain transition matrices $\mathbf{P}(k), k=1,\ldots,H$. They depend on the wavelength loads $\{u_k\}_{k=1}^H$, the sojourn probabilities in each format $\{\alpha_m\}_{m=1}^F$, and the a-priori format probabilities $\{P_m\}_{m=1}^F$. These are assumed to be the same on all wavelengths λ_p.

B.1. XCI mean

Let's first find the average sojourn time in format m. From (B.2) we get

$$E[N_m] = \sum_{k=1}^{H} E[I_k(m)]\mathcal{S}_k = \sum_{k=1}^{H} p_m^{(k)} \mathcal{S}_k \tag{B.4}$$

where $p_m^{(k)} = \mathrm{P}\{X_k = m\}$ is the probability that the chain visits state m at hop k. Let[3] $\underline{p}^{(k)} = [p_0^{(k)},\ldots,p_F^{(k)}]^T$ be the column "state vector" at "time" k. The total probability law for the Markov chain yields the Chapman–Kolmogorov update [22]

$$\underline{p}^{(k)} = \Pi^{(k,0)} \underline{p}^{(0)} \tag{B.5}$$

where $\underline{p}^{(0)}$ is the initial known distribution of the chain, and for $k \geq l$ we defined

$$\Pi^{(k,l)} \equiv \{\pi_{i,j}^{(k,l)}\} = \begin{cases} \mathbf{P}(k)\cdot\ldots\cdot\mathbf{P}(l+1) & \text{if } k>l \\ \mathbf{I} & \text{if } k=l \end{cases} \tag{B.6}$$

where $\mathbf{I}$ is the $(1+F)\times(1+F)$ identity matrix. Algorithmically, since we have the H matrices $\mathbf{P}(k)$, $k=1,\ldots,H$, then we compute $\underline{p}^{(k)} = \mathbf{P}(k)\underline{p}^{(k-1)}$ for $k=1,\ldots,H$ and store such H vectors. Then per (B.4) the weighted sum of their m-th entries yields $E[N_m]$.

Finally, from (B.3) the XCI mean is

$$\eta_a \triangleq E[a_{XCI}] = \mathcal{C}\sum_{p\neq 0}\sum_{m=1}^{F} g_{pm} E[N_{pm}]$$

$$= \mathcal{C}\sum_{p\neq 0} \underline{g}_p^T \sum_{k=1}^{H} \mathcal{S}_k \underline{\tilde{p}}^{(k)}$$

where $\underline{g}_p^T \triangleq [g_{p1},\ldots,g_{pF}]$, and $\underline{\tilde{p}}^{(k)}$ is derived from vector $\underline{p}^{(k)}$ in (B.5) by deleting the first entry. The dependence of $E[N_{pm}] \equiv E[N_m]$ on format comes from the dependence of the sojourn probability α_m on format.

B.2. XCI variance

We have from (B.3) and the assumed independence of traffic on wavelengths

$$\sigma_a^2 = \mathcal{C}^2 \sum_{p\neq 0} Var\left[\sum_{m=1}^{F} g_{pm} N_{pm}\right].$$

Using the bilinearity of the covariance

$$Var\left[\sum_{m=1}^{F} g_{pm} N_{pm}\right] = \sum_{m_1,m_2=1}^{F} g_{pm_1} g_{pm_2} Cov[N_{pm_1}, N_{pm_2}]. \tag{B.7}$$

We thus need to compute for all m_1, m_2 (omit subscript p)

$$\begin{aligned} Cov[N_{m_1}, N_{m_2}] &= Cov[\sum_{i=1}^{H} I_{m_1}(i)\mathcal{S}_i, \sum_{k=1}^{H} I_{m_2}(k)\mathcal{S}_k] \\ &= \sum_{i,k} \mathcal{S}_i\mathcal{S}_k \left(E[I_{m_1}(i)I_{m_2}(k)] - E[I_{m_1}(i)]E[I_{m_2}(k)]\right) \\ &= \underbrace{\sum_{i,k} \mathcal{S}_i\mathcal{S}_k \mathrm{P}\{X_i=m_1, X_k=m_2\}}_{\triangleq A_{m_1m_2}} \backslash - t \\ &\quad - \underbrace{\sum_i p_{m_1}^{(i)} \mathcal{S}_i \sum_k p_{m_2}^{(k)} \mathcal{S}_k}_{E[N_{m_1}]E[N_{m_2}]} \backslash - t \end{aligned} \tag{B.8}$$

where we again used the bilinearity of covariance, and $E[N_m]$ is obtained from (B.4).

Let us now concentrate on the contribution of the first term $A_{m_1m_2}$ to the variance σ_a^2. Let us compute

$$B_p \triangleq \sum_{m_2=1}^{F} g_{pm_2} \sum_{m_1=1}^{F} g_{pm_1} A_{m_1m_2}. \tag{B.9}$$

if $k \geq i$, then $\mathrm{P}\{X_i=m_1, X_k=m_2\} = \mathrm{P}\{X_k=m_2|X_i=m_1\}\mathrm{P}\{X_i=m_1\} = \pi_{m_2,m_1}^{(k,i)} p_{m_1}^{(i)}$ from the memoryless property of the Markov chain. Note that when $k=i$ we have $\Pi^{(i,i)} = \mathbf{I}$, and thus $\pi_{m_2,m_1}^{(i,i)} = \delta_{m_1,m_2}$ is a Kronecker delta. Similarly, if $k<i$, then $\mathrm{P}\{X_i=m_1, X_k=m_2\} = \mathrm{P}\{X_i=m_1|X_k=m_2\}\mathrm{P}\{X_k=m_2\} = \pi_{m_1,m_2}^{(i,k)} p_{m_2}^{(k)}$. Thus

$$B_p = \sum_{i,k=1}^{H} \mathcal{S}_i\mathcal{S}_k \sum_{m_2=1}^{F} g_{pm_2} \times \begin{cases} \displaystyle\sum_{m_1=1}^{F} \pi_{m_2,m_1}^{(k,i)} p_{m_1}^{(i)} g_{pm_1} & \text{if } k>i \\ p_{m_2}^{(k)} g_{pm_2} & \text{if } k=i \\ \left[\displaystyle\sum_{m_1=1}^{F} \pi_{m_1,m_2}^{(i,k)} g_{pm_1}\right] p_{m_2}^{(k)} & \text{if } k<i. \end{cases}$$

[3] We use here column probability vectors. Also note that p_{ij} is the transition probability from state j to state i. Such a notation is the transpose of the standard Markov chain notation [22], but is consistent with dynamic systems state-space notation in control theory.

Please cite this article as: A. Bononi, et al., Regeneration savings in flexible optical networks with a new load-aware reach maximization, Optical Switching and Networking (2015), http://dx.doi.org/10.1016/j.osn.2015.07.003

It is straightforward to verify that the sums over m_1, m_2 have simple matrix–vector multiplication interpretations. Hence

$$B_p = \underline{\mathcal{S}}^T \mathbf{M}_p \underline{\mathcal{S}} \tag{B.10}$$

where $\underline{\mathcal{S}}^T \triangleq [\mathcal{S}_1, \ldots, \mathcal{S}_H]$, and the matrix $\mathbf{M}_p \equiv \{m_{p,i,k}\}_{i,k=1}^{H}$ has elements

$$m_{p,i,k} = \begin{cases} \underline{g}_p^T \tilde{\Pi}^{(k,i)} (\underline{\tilde{p}}^{(i)} \odot \underline{g}_p) & \text{if } k > i \\ \underline{g}_p^T (\underline{\tilde{p}}^{(i)} \odot \underline{g}_p) & \text{if } k = i \\ \underline{g}_p^T \tilde{\Pi}^{(i,k)} (\underline{\tilde{p}}^{(k)} \odot \underline{g}_p) & \text{if } k < i \end{cases} \tag{B.11}$$

where $\odot$ indicates the element-wise (Hadamard) product, and $\tilde{\Pi}^{(k,l)}$ is the $F \times F$ matrix obtained from $\Pi^{(k,l)}$ by deleting the first row and first column, i.e., those corresponding to the 0 state. Thus finally,

$$\sigma_a^2 = \mathcal{C}^2 \sum_{p \neq 0} \left[\underline{\mathcal{S}}^T \mathbf{M}_p \underline{\mathcal{S}} - \left(\sum_{m=1}^{F} g_{pm} E[N_{pm}] \right)^2 \right] \tag{B.12}$$

which is easily verified to coincide with (19) at $\sigma_{gp}^2 = 0$ when spans are identical ($\mathcal{I}_k = \mathcal{S}_k \mathcal{I}^{(1)}$) and a single format ($F=1$) is allowed on each wavelength.

References

[1] O. Rival, G. Villares, A. Morea, Impact of inter-channel nonlinearities on the planning of 25-100 Gb/s elastic optical networks, J. Lightw. Technol. 29 (2011) 1326–1334.
[2] K. Christodoulopoulos, I. Tomkos, E.A. Varvarigos, Elastic bandwidth allocation in flexible OFDM-based optical networks, J. Lightw. Technol. 29 (2011) 1354–1366.
[3] E. Palkopoulou, G. Bosco, A. Carena, D. Klonidis, P. Poggiolini, I. Tomkos, Nyquist-WDM-based flexible optical networks: exploring physical layer design parameters, J. Lightw. Technol. 31 (14) (2013) 2332–2339.
[4] C. Rottondi, M. Tornatore, A. Pattavina, G. Gavioli, Traffic grooming and spectrum assignment for coherent transceivers in metro-flexible networks, IEEE Photon. Technol. Lett. 25 (2013) 183–186.
[5] G. Zhang, M. De Leenheer, A. Morea, B. Mukherjee, A survey on OFDM-based elastic core optical networking, IEEE Commun. Surv. Tutor. 15 (2013) 65–87 (1st quarter).
[6] P. Poggiolini, G. Bosco, A. Carena, R. Cigliutti, V. Curri, F. Forghieri, R. Pastorelli, S. Piciaccia, The LOGON strategy for low-complexity control plane implementation in new-generation flexible networks, in: Proceedings of OFC'13, OW1H.3, 2013.
[7] P. Johannisson, E. Agrell, Modeling of nonlinear signal distortion in fiber-optic networks, J. Lightw. Technol. 32 (23) (2014) 3942–3950.
[8] D.J. Ives, A. Lord, P. Wright, S.J. Savory, Quantifying the impact of non-linear impairments on blocking load in elastic optical networks, in: Proceedings of OFC'14, paper W2A.55, 2014.
[9] A. Bononi, P. Serena, G. Picchi, A. Morea, Load-aware transparent reach maximization in flexible optical networks, in: Proceedings of NOC'14, paper s8.1, pp. 165-172, Milan, Italy, 2014.
[10] P. Poggiolini, The GN model of non-linear propagation in uncompensated coherent optical systems, J. Lightwave Technol. 30 (2012) 3857–3879.
[11] P. Johannisson, M. Karlsson, Perturbation analysis of nonlinear propagation in a strongly dispersive optical communication system, J. Lightw. Technol. 31 (8) (2013) 1273–1282.
[12] A. Bononi, P. Serena, An alternative derivation of Johannisson's regular perturbation model (2012), arXiv:1207.4729v1[physics.optics].
[13] E. Grellier, A. Bononi, Quality parameter for coherent transmissions with Gaussian-distributed nonlinear noise, OSA Opt. Expr. 19 (13) (2011) 12781–12788.
[14] P. Poggiolini, A. Carena, V. Curri, G. Bosco, F. Forghieri, Analytical modeling of non-linear propagation in uncompensated optical transmission links, IEEE Photon. Technol. Lett. 23 (11) (2011) 742–744.
[15] A. Bononi, N. Rossi, P. Serena, On the nonlinear threshold versus distance in long-haul highly-dispersive coherent systems, OSA Opt. Expr. 20 (26) (2012) B204–B216.
[16] A. Bononi, O. Beucher, P. Serena, Single- and cross-channel nonlinear interference in the Gaussian Noise model with rectangular spectra, OSA Opt. Expr. 21 (26) (2013) 32254–32268.
[17] P. Serena, A. Bononi, An alternative approach to the Gaussian noise model and its system implications, J. Lightw. Technol. 31 (22) (2013) 3489–3499.
[18] A. Bononi, N. Rossi, P. Serena, Performance dependence on channel symbol rate of coherent single-carrier WDM systems, in: Proceedings of ECOC'13, paper Th.1.D.5, 2013.
[19] A. Morea, N. Brogard, F. Leplingard, J.-C. Antona, T. Zami, B. Lavigne, D. Bayart, QoT function and A* routing: an optimized combination for connection search in translucent networks, J. Opt. Netw. 7 (2008) 42–61.
[20] P. Péloso, D. Penninckx, M. Prunaire, L. Noirie, Optical transparency of a heterogeneous pan-European network, J. Lightw. Technol. 22 (2004) 242–248.
[21] W. Shi, Z. Zhu, M. Zhang, N. Ansari, On the effect of bandwidth fragmentation on blocking probability in elastic optical networks, Trans. Commun. 61 (7) (2013) 2970–2978.
[22] A. Leon-Garcia, Probability, Statistics, and Random Processes for Electrical Engineering, 3rd ed., Prentice-Hall, Upper-Saddle River, 2008.

Please cite this article as: A. Bononi, et al., Regeneration savings in flexible optical networks with a new load-aware reach maximization, Optical Switching and Networking (2015), http://dx.doi.org/10.1016/j.osn.2015.07.003